Robust Airfoil Optimization in High Resolution Design Space

Wu Li and Sharon L. Padula

NASA Langley Research Center, Hampton, Virginia, USA
w.li@larc.nasa.gov

1. Abstract

The robust airfoil shape optimization is a direct method for drag reduction over a given range of operating conditions and has three advantages: (1) it prevents severe degradation in the off-design performance by using a smart descent direction in each optimization iteration, (2) it uses a large number of B-spline control points as design variables yet the resulting airfoil shape is fairly smooth, and (3) it allows the user to make a trade-off between the level of optimization and the amount of computing time consumed. The robust optimization method is demonstrated by solving a lift-constrained drag minimization problem for a two-dimensional airfoil in viscous flow with a large number of geometric design variables.

Our experience with robust optimization indicates that our strategy produces reasonable airfoil shapes that are similar to the original airfoils, but these new shapes provide drag reduction over the specified range of Mach numbers. We have tested this strategy on a number of advanced airfoil models produced by knowledgeable aerodynamic design team members and found that our strategy produces airfoils better or equal to any designs produced by traditional design methods.

2. Keywords: shape optimization, CFD, optimization under uncertainty

3. Introduction

The present research seeks optimization methods that are robust in the sense that they produce solutions insensitive to changes in the input parameters. Furthermore, the methods must be able to find solutions by using a moderate number of high-fidelity disciplinary analyses. This second requirement acknowledges the fact that disciplinary analyses (e.g., computational fluid dynamics (CFD)) can be computationally expensive; an optimization method that requires thousands of function evaluations has limited usefulness in the current design environment. Finally, there is a need for a conservative approach that achieves a robust design in the neighborhood of a baseline configuration. This approach is useful to the design team that has a good baseline design developed by traditional methods.

The concept of robust optimization is demonstrated by using a 2-D airfoil shape optimization problem. Hicks and Vanderplaats studied a simplified version of this airfoil problem in 1977 [1]. For example, consider Fig. 1, reproduced from Ref. 1. Hicks and Vanderplaats demonstrate that a direct optimization approach that minimizes drag at one Mach number (e.g., $M = 0.75$) actually increases drag at nearby Mach numbers (e.g., $M = 0.70$). The authors also present evidence showing that an inverse optimization approach that adjusts the airfoil shape to match some ideal pressure distribution will display similar point-optimization behavior. The conclusion is that changes in airfoil shape that are advantageous at one Mach number may cause poor performance at other Mach numbers. This result is especially apparent for supercritical airfoil designs because the relationship between wave drag and free stream velocity is quite nonlinear for high subsonic design Mach numbers.

To overcome off-design performance degradation, many authors have proposed variations of multipoint optimization [2–5]. However, minimizing a weighted sum of objective functions can produce many different solutions, depending on the choice of the weights and the number and spacing of the multiple design points. Also, there is no guarantee that any of the solutions will yield desirable airfoil shapes [2, 3]. Moreover, several authors suggest that if the number of design points n is much smaller than the number of design variables m (i.e., $n << m$), the resulting airfoil will be misshapen [2–4].

Li, Padula, and Huyse discuss the shortcomings of multipoint optimization and propose new robust optimization algorithms [4, 6]. The goal of robust optimization is to find the airfoil shape that minimizes the mean of the drag coefficient over a range of free-stream Mach numbers, $M_{\min} < M < M_{\max}$, and keeps the performance fluctuation as low as possible. The standard robust optimization model of minimizing the mean and the variance can be used for this purpose:

$$\min_{\Delta D, \Delta\alpha} \left(E(C_d), \sigma^2(C_d) \right) \tag{1}$$

subject to

$$C_l(D, \alpha, M) = C_l^* \quad \text{for all } M, \tag{2}$$

where C_l^* is the required lift, D is a set of m airfoil geometric design variables, C_l is the lift coefficient, and C_d is the drag coefficient. Both C_l and C_d are functions of angle of attack α and free-stream Mach number M. Note that α is the angle of attack that satisfies Eq.(2) for each M. The mean and variance of C_d are defined as follows:

$$E(C_d) = \int_{M_{\min}}^{M_{\max}} C_d(D,\alpha,M)\,p(M)\,dM \tag{3}$$

$$\sigma^2(C_d) = \int_{M_{\min}}^{M_{\max}} \left(C_d(D,\alpha,M) - E(C_d)\right)^2 p(M)\,dM \tag{4}$$

where *p(M)* is the probability density function of *M*. In this paper, we choose a uniform distribution to capture the fact that the design team desires a simultaneous reduction in drag over the range of Mach numbers. Ref. 4 discusses other choices of *p(M)*.

One attractive option for solving the 2-D airfoil problem is presented in Ref. 6, which uses the CFD analysis of Ref. 7. The former research demonstrates the potential importance of robust airfoil optimization but solves a simplified problem by choosing the Euler inviscid option in the CFD analysis code, a poor initial guess, a coarse 2-D unstructured grid, and no airfoil thickness constraints. The present study will test the robust optimization method with a larger number of design variables, viscous CFD analysis, a finer grid, a good initial guess, and realistic design constraints.

4. General Solution Strategy

The robust airfoil optimization strategy consists of the following steps:

1. Select *n* Mach numbers, $M_1, M_2, \ldots, M_n$.
2. Find the smallest feasible angle of attack for each Mach number.
3. Calculate lift, drag, and their gradients.
4. Formulate a linear subproblem.
5. Adjust the trust region step size to achieve predetermined drag reduction.
6. Solve the linear subproblem and update values of design variables.
7. Decide whether to terminate or iterate from step 1.

The methods described in Refs. 4 and 6 are similar to each other but differ in steps 1, 4, 5, and 6. In this paper, we will demonstrate the method described in Ref. 6.

Step 1 in the general strategy can vary in the number of Mach points selected and in the method of selection. Ref. 4 favors a random selection of Mach points in order to avoid the point-optimization phenomenon. Ref. 6 favors a fixed set of Mach points because the convergence properties associated with randomly selected points are difficult to anticipate. The Mach points M_i are selected from a range [0.68, 0.77] for all results presented in this paper. The nominal set of points is {0.68, 0.71, 0.74, 0.76}. The range $M_i \in [0.68, 0.77]$ is selected because it contains typical cruise Mach numbers for commercial transports. The specific points are the same as those chosen by Drela [2].

Step 2 involves a line search for the smallest value of α which satisfies the lift constraint at each of the selected Mach points. This task is simple because the relationship between C_l and α is quite linear. On the first iteration, a line search is always necessary. For subsequent iterations, the linear subproblem usually provides very accurate estimates of the values of the smallest feasible α, and a line search is therefore unnecessary.

Step 3 is the calculation of the lift and drag at the design points, and their derivatives with respect to changes in geometric design variables and the angles of attack.

Step 4 involves formulating the linear subproblem. Of all the possible solutions to the linear subproblem, we seek the one that minimizes the drag at all the design conditions simultaneously and proportionally while making the smallest change in the design vector in a least norm sense. The linear subproblem can be summarized as:

$$\min_{\Delta D, \Delta\alpha} \max_{1 \le i \le n} \frac{C_{d,i}^{new}}{C_{d,i}} \tag{5}$$

subject to:

$$C_{d,i}^{new} = C_{d,i} + \left\langle \frac{\partial C_{d,i}}{\partial D}, \Delta D \right\rangle + \frac{\partial C_{d,i}}{\partial \alpha_i}\Delta\alpha_i \tag{6}$$

$$C_{l,i} + \left\langle \frac{\partial C_{l,i}}{\partial D}, \Delta D \right\rangle + \frac{\partial C_{l,i}}{\partial \alpha_i}\Delta\alpha_i = C_l^* \qquad \text{for } 1 \le i \le n \tag{7}$$

$$-\delta_j \le \Delta D_j \le \delta_j \qquad \text{for } 1 \le j \le m \tag{8}$$

along with some geometric constraints.

Here the notation $< a, b >$ indicates the dot product of vectors a and b, $C_{d,i}$ is the current value of the drag coefficient evaluated at the i^{th} design point, and $C_{d,i}^{new}$ is the linear prediction to the value of $C_{d,i}$ after the optimization step. The additional geometric constraints can be

tailored to meet the needs of the design team. In this paper, geometric constraints are used to enforce the desired airfoil thickness at spar locations and at the maximum thickness location. Also, the bounds δ_j are adjusted in step 5 to set the trust region size.

This linear subproblem seeks a smart descent direction that reduces each individual $C_{d,i}$ to achieve a reduction of the mean and variance of the drag.

Step 5, the determination of trust region step size, is crucial and requires the most explanation (see Ref. 6 for complete details). The size of each optimization step is controlled by a tuning parameter $\gamma_{\min}$, which specifies the desired decrease in C_d at each design point. Because the computational cost of solving the approximate optimization subproblem is inexpensive compared with the cost of CFD analysis, the subproblem can be solved with several different values of trust region size δ and then the final trust region size can be adjusted to satisfy this additional constraint:

$$\max_{1 \le i \le n} \frac{C_{d,i}^{new}}{C_{d,i}} = 1 - \gamma_{\min} \tag{9}$$

In this paper, $\gamma_{\min} = 0.03$. The setting is recommended in Ref. 6 and appears to be a good compromise between rapid convergence and an attainable rate of decrease. Ref. 8 discusses the use of this parameter to meet the needs of a design team.

Step 6 involves the solution of the approximate optimization subproblem and the update of the design variable values. The current paper uses a quadratic programming solver to find the least norm solution of the linear program given in Eqs.(5)–(9).

Ideally, step 7 uses a termination criterion based on the comparison between the predicted decrease and the actual decrease delivered by step 6. For the purpose of demonstrating the technology, we set the maximum number of iterations based on the number of CFD analyses that we could afford. Therefore, step 7 is not implemented.

The algorithm described in steps 1–7 is very similar to sequential linear programming; however, it has three key unconventional elements. These elements are employed to find a smart search direction that takes into account the fact that only a limited amount of information (i.e., the drag at a few design points) is given for solving the robust optimization problem. The unconventional elements are: (1) a predetermined rate of linearized drag reduction to ensure a proper trust region size, (2) the adaptive minimax formulation to ensure simultaneous drag reduction at all the design points, and (3) the least norm solution of the linear programming subproblem for an efficient trade-off between the shape modification and the performance improvement. The combination of these three elements yields fairly smooth airfoils during optimization and prevents severe off-design performance degradation.

5. Results and Conclusions

The lift-constrained 2-D airfoil optimization problem stated in Eqs.(1) and (2) is used to test the robust optimization approach. The general optimization strategy is tested on a realistic airfoil design by solving fully turbulent Navier-Stokes equations and the corresponding discrete adjoint equations. The initial RAE2822 airfoil is shown in Fig. 2. Thirty-five bounded geometric design variables, D_j, shown as circles in Fig. 3, are the B-spline control points used to create a wide variety of smooth 2-D airfoil shapes. The leading edge and trailing edge points are fixed so that the chord length does not change, but the y coordinates of the top and bottom surfaces can change as long as the lift constraint given in Eq. (2) is satisfied. Additional constraints on D_j are included so that the maximum airfoil thickness does not decrease, the thickness at two spar locations is maintained, and the spline points near the trailing edge change smoothly.

Figures 4–7 show typical optimization results for the case where $p(M)$ is a uniform distribution. Fig. 4 shows the change in drag with optimization iteration at the four design points. These 10 optimization iterations required approximately 100 calls to the full CFD and sensitivity analysis code. Notice that each optimization iteration yields some improvement; thus, the method is applicable even when the CFD analysis is computationally expensive. Note that the points plotted in Fig. 4 represent the solutions to viscous CFD analyses not the drag counts predicted by linear approximation (i.e., Fig. 4 shows $C_{d,i} \times 10^4$ rather than $C_{d,i}^{new} \times 10^4$). Similarly in Fig. 5, drag profiles are plotted before and after 10 iterations of the general strategy. Drag counts for the 10^{th} iterate are obviously less than those for the original airfoil, although both airfoils provide the required lift, $C_l^* = 0.733$. Fig. 5 shows that drag is reduced at the four design points (i.e., M_i = 0.68, 0.71, 0.74, 0.76). More significantly, Fig. 5 shows that drag is reduced at off-design points that are not sampled during the optimization strategy. The improvement is greatest at the highest Mach number and more modest near $M = 0.74$, which is the design Mach number for the original airfoil. Fig. 6 shows the difference in shape between the original and the optimized airfoil. The dashed vertical lines indicate the chordwise position of thickness constraints. The first and third vertical lines correspond to the location of structural spars and the middle line indicates the maximum thickness location. In these three locations, the y coordinates of the airfoil may change, but the distance from the bottom to the top of the airfoil does not change. Finally, Fig. 7 shows the pressure distributions before and after 10 optimization iterations. This plot indicates that the drag reduction is due to significant changes in pressure distribution caused by small changes in the airfoil shape. Only the pressure distribution at $M = 0.76$ is reproduced, although the other pressure distributions were examined and exhibit similar characteristics.

Our experience with the general solution strategy is that it produces reasonable airfoil shapes that are similar to the original airfoils, and it provides consistent drag reduction over the specified range of Mach numbers. We have tested this strategy on a number of advanced airfoil models produced by knowledgeable aerodynamic design team members. We have been able to provide improved designs that met all the criteria established by the teams. The improved designs were evaluated by using more than one CFD analysis code and proved to be better or equal to any designs produced by traditional design methods. In working with the aerodynamic teams, we discovered that the optimization strategy reported herein can be modified to give the user more control over the outcome. Ref. 8 contains a thorough discussion of those modifications.

The robust optimization strategy has been demonstrated for an optimization problem with one uncertain parameter, cruise Mach number. The authors believe that this strategy can be extended to problems with several uncertain parameters. The challenge is to predict the expected decrease in the drag with a limited number of expensive disciplinary analyses. One approach is to screen the candidate uncertain parameters and fix the values of parameters that have a less significant effect on the objective. Another approach is to use an efficient sampling scheme such as Latin hypercube sampling. These approaches should be successful as long as the lift and drag information at the sampled points reflects the overall trend of lift and drag.

It is concluded that robust optimization is an important tool for multidisciplinary design. It is useful when some of the design parameters (e.g., operating conditions) are inherently variable, when some of the design specifications are uncertain (e.g., maximum payload), or when some of the cost drivers are subject to change in the future (e.g., fuel prices). The importance of robust optimization increases when these uncertain parameters have a strong nonlinear effect on the objective function and constraints. An interesting example of robust optimization is provided in this demonstration of airfoil shape optimization. In the example problem, cruise Mach number is the uncertain operating condition with nonlinear effects on lift and drag of the airfoil.

6. References

1. Hicks R M and Vanderplaats G N. Application of numerical optimization to the design of supercritical airfoils without drag-creep. SAE Paper 770440, Business Aircraft Meeting, Wichita, 1977
2. Drela M. Pros and cons of airfoil optimization. Frontiers of CFD 1998, eds. Caughey and Hafez, World Scientific, 1998, 363–381
3. Reuther J A, Jameson A, Alonso J J, Rimlinger M J, and Saunders D. Constrained multipoint aerodynamic shape optimization using adjoint formulation and parallel computers, Part 1 & 2. AIAA J. Aircr., 1999, 36(1):51–74
4. Huyse L, Padula S L, Lewis R M, and Li W. A probabilistic approach to free-form airfoil shape optimization under uncertainty. AIAA J., 2002, 40(9):1764–1772
5. Nemec M, Zingg D W, and Pulliam T H. Multi-point and multi-objective aerodynamic shape optimization. AIAA Paper 2002-5548, 9th AIAA/ISSMO Symposium on Multidisciplinary Analysis and Optimization, Atlanta, 2002
6. Li W, Huyse L, and Padula S. Robust airfoil optimization to achieve drag reduction over a range of Mach numbers. Struc. & Multi. Opt., 2002, 24(1):38–50
7. Anderson W K and Bonhaus D L. Airfoil design on unstructured grids for turbulent flows. AIAA J., 1999, 37(2):185–191
8. Li W and Padula S. Performance trades study for robust airfoil shape optimization. AIAA Paper 2003-3790, To be presented at AIAA 21st Applied Aerodynamics Conference, Orlando, 2003

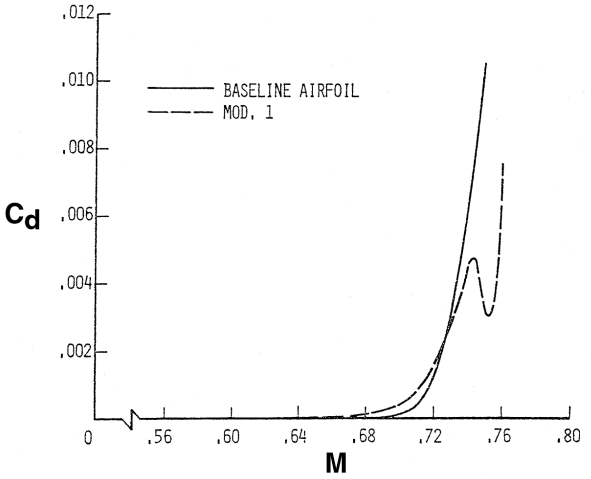

Figure 1. Drag profiles for baseline and modified airfoil (reproduced from Hicks and Vanderplaats, 1977)

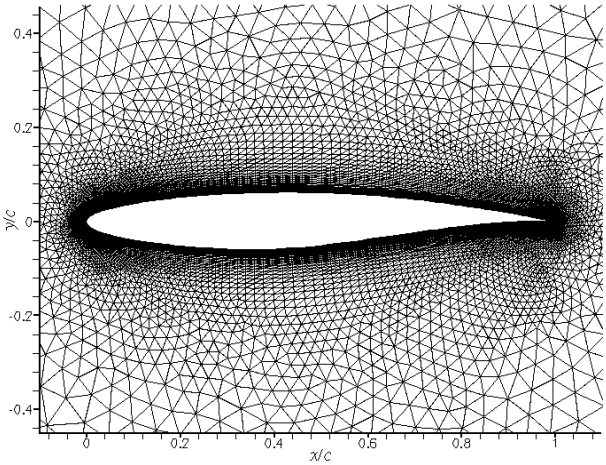

Figure 2. Grid used to solve Navier-Stokes equations

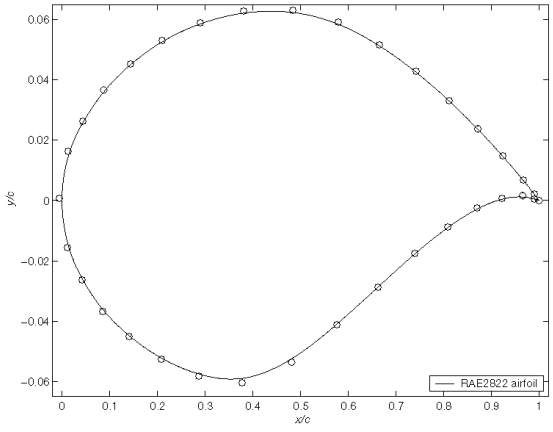

Figure 3. Parameterization of RAE2822 airfoil by cubic B-splines indicating 35 control points

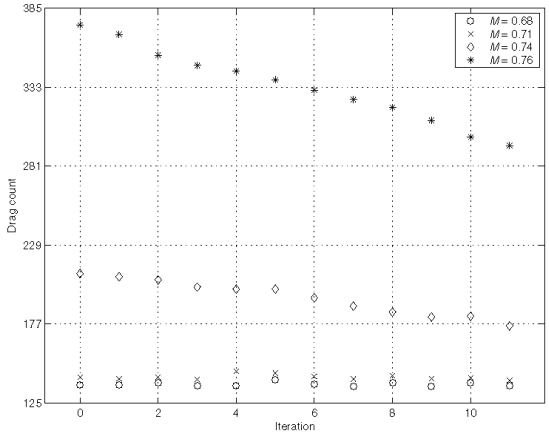

Figure 4. History of drag reduction at the four design Mach numbers

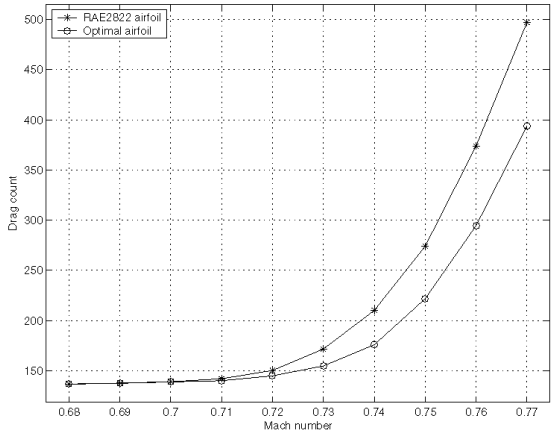

Figure 5. Postoptimization predictions of drag reduction over the specified Mach range

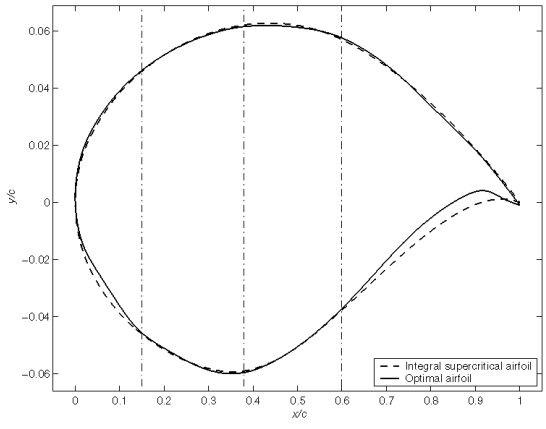

Figure 6. Optimized airfoil shape compared with original RAE2822 airfoil

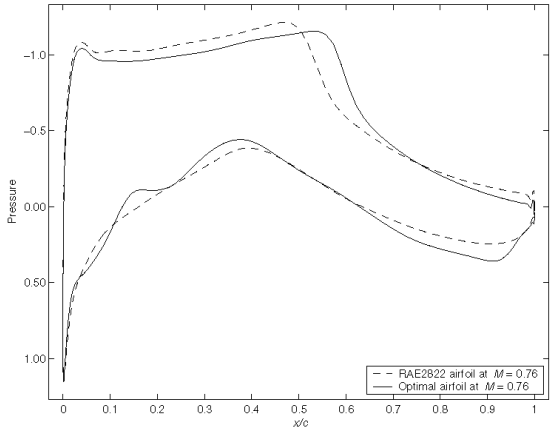

Figure 7. Pressure distributions on RAE2822 and optimized airfoil for highest Mach number design point